Conf. 781113--28

MULTIPLE ELECTRON LOSS CROSS SECTIONS FOR HEAVY IONS INCIDENT ON VARIOUS ATOMIC AND MOLECULAR GASES*

P. D. Miller†

Oak Ridge National Laboratory
Oak Ridge, Tennessee 37830

SUMMARY

Differential cross sections for charge change resulting from the scattering of 20 MeV $^{127}I^{5+}$ and 20 MeV $^{35}Cl^{4+}$ ions from thin gaseous targets have been measured.[1] Total cross sections for multiple electron loss have been determined by integration of the differential charge state yields over angle. Cross sections will be presented for $^{127}I^{5+}$ ions and $^{35}Cl^{4+}$ ions on Xe, Ar, and N_2. Impact parameter analyses of charge fraction data have been performed; these analyses depend on the assumed interatomic potential but not on any absolute measurements. The applicability of Bohr, Thomas-Fermi, and Lenz-Jensen potentials with the experimental total cross sections will be shown. A different method, using a magnetic quadrupole to focus individual charge states, was used to measure absolute charge state yields of 20 MeV Fe ions emerging within a large acceptance angle from a differentially pumped gas cell of length 9.4 cm.[2] N_2, Ar, Kr, Xe, and SF_6 targets were investigated. From the low pressure yields total cross sections for single and multiple electron loss were obtained using an improved version of the initial growth method.

I. INTRODUCTION

Charge changing cross sections for heavy ions incident on molecules and atoms are a rich source of information on the dynamics of collisional processes. These cross sections are so large that only gas targets may be made sufficiently dilute to be able to make measurements under single collision conditions. Considerable experimental information is available for light ions,[3] and the available data for heavier ion total cross sections has been comprehensively reviewed by Betz.[4] However, very few absolute differential cross sections have been measured, and for much of the older data on absolute total cross sections, the solid angle for acceptance of the charge state analysis system was insufficient to collect all of the particles populating the higher charge states. The available data on differential and total electron capture and loss processes has been summarized and referenced in previous publications.[1,2]

In Sect. II, we present differential cross sections for 20 MeV I^{5+} and Cl^{4+} ions incident on Xe, Ar, and N_2 targets. We use the classical correspondence between scattering angle and impact parameter to display the impact parameter dependence of charge state fractions and predict the total charge changing cross sections. By comparing these cross sections with those obtained by direct integration of the absolute yields over angle, we obtain a sensitive test of the assumed interatomic potential. The applicability of Bohr, Thomas-Fermi, and Lenz-Jensen potentials is discussed.

In Sect. III, we present measurements of absolute charge state yields of 20 MeV Fe ions emerging from gaseous targets of N_2, Ar, Kr, Xe, and SF_6. The acceptance solid angle of the charge state analysis system was made sufficiently large, by using a magnetic quadrupole doublet, so that essentially all particles entering the target were counted. The pressure in the differentially pumped gas cell of length 9.4 cm ranged from 2 to 400 mTorr, thereby covering both the low pressure region where single events dominate the charge change as well as the high pressure region where equilibrium conditions are met. From the low pressure yields, we have calculated the total cross sections for loss of one electron and of multiple electrons in a single event and the cross section for loss of the initial charge state, which in this experiment was +4. The method used for obtaining the cross sections was an improved version of the 'initial growth' technique.

II. ANGULAR DIFFERENTIAL CROSS SECTION MEASUREMENTS AND POTENTIAL MODEL ANALYSIS FOR 20 MeV Cl^{4+} AND I^{5+} IONS INCIDENT ON THIN GASEOUS TARGETS

The experimental apparatus is virtually identical to that reported earlier.[5] A momentum analyzed 20 MeV ion beam of either $^{127}I^{5+}$ or $^{35}Cl^{4+}$, produced in the ORNL tandem accelerator, was collimated prior to entering a differentially pumped gas cell by two apertures, separated by 10 meters, with diameters of 1.25 mm and 0.5 mm, respectively. The cell was positioned 27 cm after the second defining aperture and mounted directly above a 1400 ℓ/sec diffusion pump; it consisted of two circular entrance apertures, each 1 mm in diameter, and two exit slot apertures 1 x 2.5 mm and 1 x 4 mm. All apertures were spaced 2 cm apart. The slotted exit apertures permitted observation at scattering angles up to 3°. Target gases were introduced at the center of the gas cell. Target pressures were measured with a capacitance manometer. Charged particles scattered at a given angle were separated according to their charge with an electrostatic analyzer located ~3 m from the target, and were recorded using a position sensitive solid state detector.

In order to obtain absolute differential charge changing cross sections, incident beam intensity, gas target thickness, and solid angle information are required. A surface barrier detector, used to detect particles multiply scattered at 60° from a chemically etched annular Ni film situated between the two defining apertures, served as the incident beam intensity monitor.[6] Calibration of the monitor system provided a direct way of measuring the number of particles entering the target.

The total charge changing cross sections were determined by integrating the absolute yields over angle and employing the thin target relation

$$\sigma(q_i,q) = \frac{1}{Nt} \int Y_q(\Omega)d\Omega \quad \text{for } q \neq q_i \qquad (1)$$

*Research sponsored by the Division of Physical Research, U.S. Dept. of Energy, under contract W-7405-eng-26 with Union Carbide Corporation.

†With G.D. Alton, A. Antar, L.B. Bridwell, C.M. Jones, Q. Kessel, H. Knudsen, C.D. Moak, R.O. Sayer, and H.A. Scott.

where $Y_q(\Omega)$ is the measured absolute yield per incident particle per unit solid angle, N is the number density of the target gas and t is the length of the gas cell. For absolute yield measurements, the single collision criterion is that the yields increase linearly with target thickness and thus give constant cross section values for the lowest target thicknesses. The range of target thicknesses for which this condition is met varies with the final charge state. Single electron capture cross sections $\sigma(q,q-1)$ have been found to increase sharply with ionic charge.[4] To avoid depletion of high charge state populations through electron capture after the initial collision in which the high charge states are produced, a thinner target is necessary than for low charge states. The experimentally determined cross sections $\sigma(q_i,q)$ for 20 MeV ^{127}I with $q_i = 5$ and 20 MeV ^{35}Cl with $q_i = 4$ remained constant to within ~ 10% for cell pressures up to 20 mTorr for $q < 15$, indicating that the single-collision criterion was satisfied. For $q \geq 15$ (only observed with ^{127}I), the onset of an apparent decrease in $\sigma(5,q)$ with pressure indicated where the single collision criterion was not satisfied. Only data from the linear regions were used for cross section calculations.

At each laboratory scattering angle θ_ℓ, a complete charge state distribution was recorded so that charge state fractions $f_q(\theta_\ell)$ could be derived. If these charge state fractions are expressed as a function of impact parameter p, instead of scattering angle θ_ℓ, then the total charge changing cross section, $\sigma(q_i,q)$ can be obtained from the following expression

$$\sigma(q_i,q) = 2\pi \int_0^\infty f_q(p)pdp. \qquad (2)$$

The classical correspondence between center-of-mass scattering angle θ and impact parameter p for scattering by a central potential V(r) is given by[7]

$$\theta = \pi - 2\int_{r_0}^{\infty} \frac{p/r^2}{[1 - p^2/r^2 - V(r)/E]^{\frac{1}{2}}}\,dr \qquad (3)$$

where E is the center-of-mass energy, r is the internuclear distance, and r_0 is the distance of closest approach. For a screened Coulomb potential of the form

$$V(r) = \frac{Z_1Z_2e^2}{r}\,u(r/a) \qquad (4)$$

where Z_1 and Z_2 are the atomic numbers of the colliding atoms, e is the electronic charge, u is the screening function, and a is the electronic screening length, it is possible to scale the collision parameters to produce a universal relation equivalent to Eq. (3) for all colliding atoms at nonrelativistic energies. Introducing the reduced energy

$$\epsilon = \frac{a}{Z_1Z_2e^2}\,E \qquad (5)$$

it follows that θ is a function of ϵ and p/a only. A perturbation treatment for small forward angles[8] shows that the reduced scattering angle $\bar{\theta} = \epsilon\theta/2$ is a function of the parameter p/a alone. Universal relations between reduced scattering angle $\bar{\theta}$ and p/a for Rutherford scattering and three common screening functions, corresponding to Bohr, Thomas-Fermi, and Lenz-Jensen potentials have been calculated. The calculations for the Bohr potential, which are based upon the exponential screening function

$$u(r/a) = \exp\{-r/a_B\}, \qquad (6)$$

where

$$a_B = a_o(Z_1^{2/3} + Z_2^{2/3})^{-\frac{1}{2}} \text{ and } a_o = 0.529 \times 10^{-8} \text{ cm}$$

were made using the method of Everhart *et al.*[9] The calculations with Thomas-Fermi and Lenz-Jensen potentials, where $a = 0.8853a_B$, are due to Lindhard *et al.*[8]

For each of the incident ion/target combinations used in the experiments reported here, the charge state fractions f_q were plotted as a function of impact parameter for cell pressures between 2 and 50 mTorr. For single-collision conditions, the charge state fractions obtained for an ion-target combination must be identical for the lowest cell pressures within experimental uncertainties. Only the data satisfying this requirement were used in the analyses. Charge state fractions resulting from 20 MeV $^{127}I^{5+}$ ions incident on Xe (5 mTorr) are displayed in Fig. 1. Figure 2 presents charge state fractions resulting from 20 MeV $^{35}Cl^{4+}$ ions incident on Ar (5 mTorr). The impact parameter values used for the abscissae in Figs. 1 and 2 were determined by assuming a Thomas-Fermi potential. The impact parameter resolutions corresponding to the angular resolutions used in the experiment were such that the uncertainties in impact parameter were always less than 10%. The vertical bars in Figs. 1 and 2 represent statistical uncertainties.

It can be seen from Fig. 1 that the yield of charge state 20 is primarily determined by impact parameters near 0.1Å, while the yield of charge state 10 is primarily determined by impact parameters in the neighborhood of 0.5 - 0.6 Å. These impact parameter regions are in turn sensitive to the assumed potential in regions of the same radii. Consequently, the yields of successive charge states provide a sensitive measure of the correctness of the radial dependence of the potential assumed in Eq. (2). Comparison of the total cross sections for electron loss from direct integration of the angular distributions (Eq. (1)) with those obtained from assumed potentials using Eq. (2), are shown in Figs. 3 and 4 for I^{5+} and Cl^{4+} incident on the indicated targets.

Although the Bohr potential has been used extensively for impact parameter analyses, it is known to be unsatisfactory for collisions involving impact parameters larger than about three times the screening radius. The Thomas-Fermi and Lenz-Jensen interatomic potentials provide somewhat better descriptions. Both of these potentials have been formulated for neutral collision partners. Examination of the curves shown in Figs. 3 and 4 indicates that the potentials used in processing the charge fraction data tend to underestimate the total cross sections, especially for low charge states. In all cases, the Rutherford potential leads to cross sections which are far above the measured values, therefore, it seems that a potential which takes account of the fact that the interacting particles are not neutral would be more appropriate. For example, in the case of I on Xe, the iodine ions have charge 5 and the Xe atom is neutral during approach and the emerging iodine ion may have charge 15, therefore, it is reasonable to expect that the xenon atom would also be ionized to a comparable degree. Work is in process to construct potentials which will give better agreement with the measured cross sections.

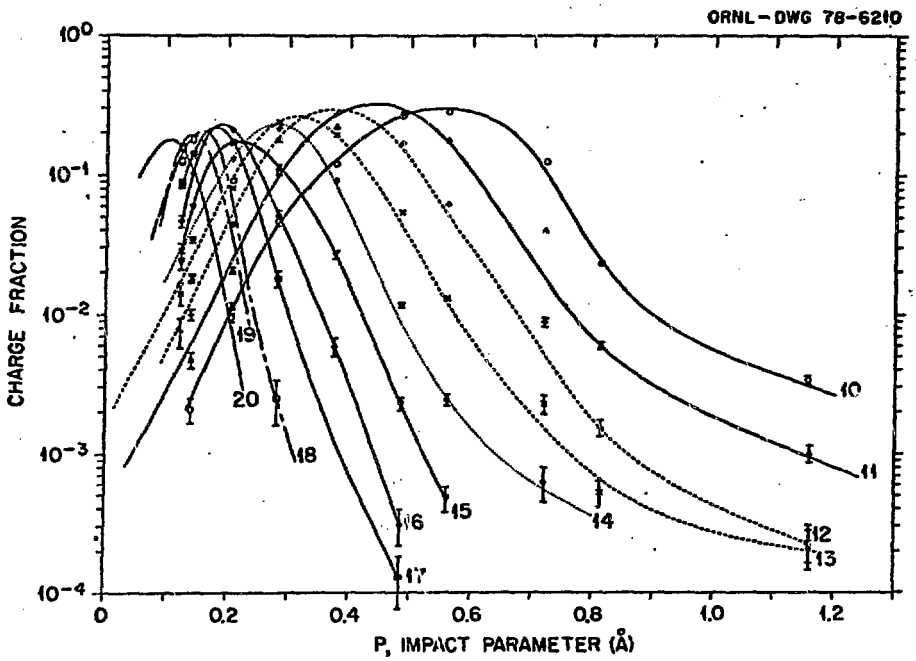

Fig. 1 - Charge state fractions vs Thomas-Fermi impact parameter for 20 MeV $^{127}I^{5+}$ incident on Xe (5 mTorr, 2 cm gas cell). $10 \leq q \leq 20$. Bars indicate statistical uncertainties.

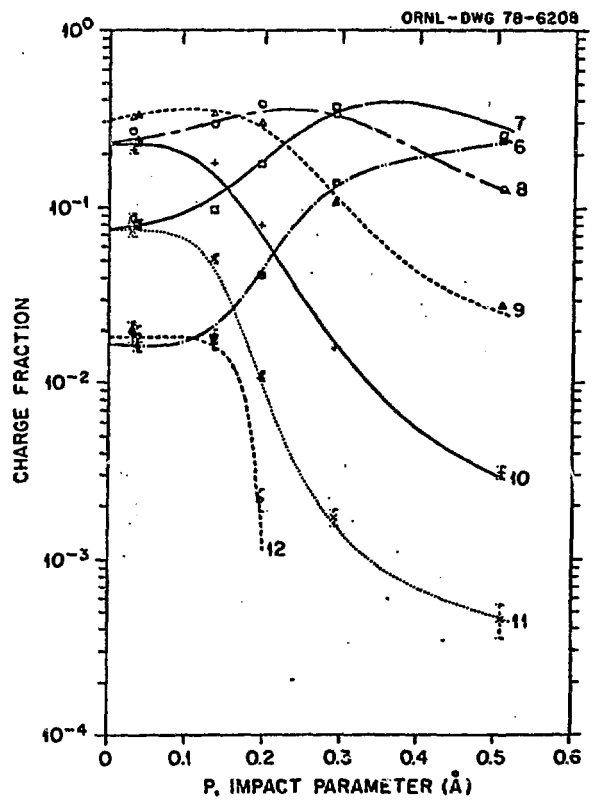

Fig. 2 - Charge state fractions vs Thomas-Fermi impact parameter for 20 MeV $^{35}Cl^{4+}$ incident on Ar (5 mTorr, 2 cm gas cell). $6 \leq q \leq 12$. Bars indicate statistical uncertainties.

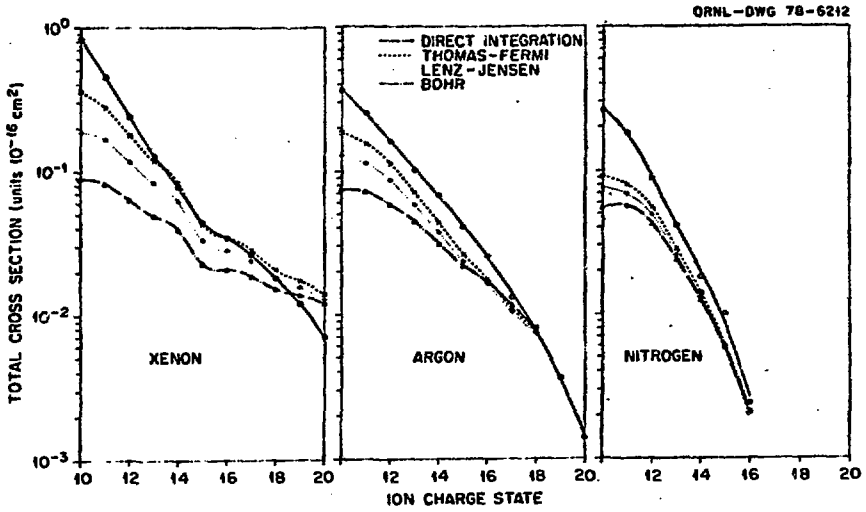

Fig. 3 - Electron loss cross sections $\sigma(5,q)$ for 20 MeV $^{127}I^{5+}$ on Xe, Ar, and N_2. Symbols refer to means of determining cross sections. The open circles (0) were derived from the integration of measured absolute differential cross sections. Points were derived from Eq. (2) with Bohr (Δ), Thomas-Fermi (x), and Lenz-Jensen (+) potentials. Lines are drawn to facilitate comparisons.

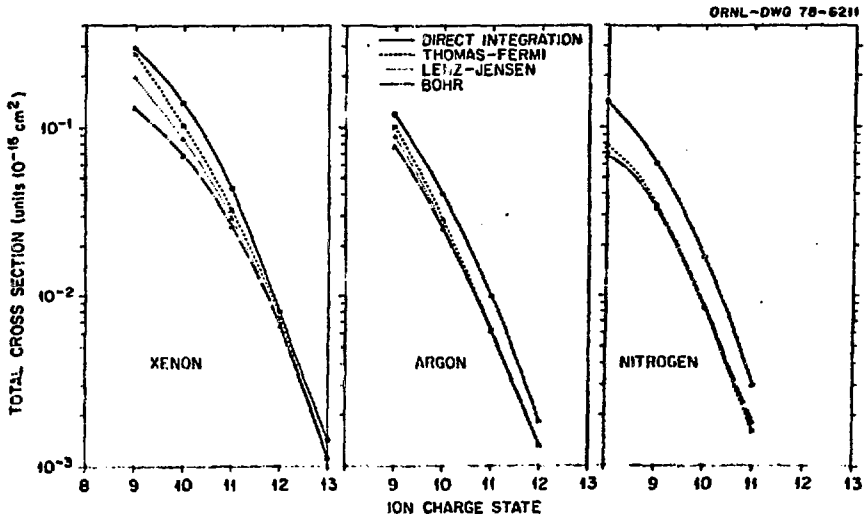

Fig. 4 - Electron loss cross sections $\sigma(4,q)$ for 20 MeV $^{35}Cl^{4+}$ on Xe, Ar, and N_2. Symbols refer to means of determining cross sections. The open circles (0) were derived from the integration of measured absolute differential cross sections. Points were derived from Eq. (2) with Bohr (Δ), Thomas-Fermi (x), and Lenz-Jensen (+) potentials. Lines are drawn to facilitate comparisons.

III. TOTAL ELECTRON LOSS CROSS SECTIONS FOR 20 MeV Fe^{4+} IONS TRANSMITTED THROUGH GASEOUS TARGETS.

The apparatus used for these measurements was similar to that described in the previous section but was modified to include a quadrupole doublet as described in Ref. 2. This doublet lens was used to focus ions of a selected charge state at the position sensitive detector which follows the charge state analyzer. Because of power supply limitations, the quadrupole lens could not focus charge states below +7. However, at low gas pressures, the scattering in the cell was so small, and the angular distributions are so peaked forward that all low-charge-state peaks were well resolved and totally collected, and therefore, these yields could be measured accurately with the lens set to focus charge +7. The spectra were very similar to those shown in Fig. 2 of Ref. 10. Count rates in the position sensitive detector were held to ∿1000 CPS, so as to minimize spectral distortion and deadtime.

For all of the target gases and gas pressures used in this experiment except Xe, we found no difference between the absolute yields obtained using 4 and 8 mrad acceptance angles. In the case of Xe-gas, which was the heaviest of the target gases used, we observed ∿10% lower yields using the 4 mrad aperture for the highest charge states (+13, +14, and +15). Because of this small difference, we feel confident that the 8 mrad acceptance angle is sufficiently large to accept virtually all particles emerging from the gas cell.

The pressure in the beam line was kept below 3×10^{-6} Torr for all pressures used in measuring cross sections. This assured a rather pure beam of charge state +4 ions. However, with no target gas in the cell, we found small traces of +5, +6, +7, and higher charge state ions of 2.2%, 1.0%, 0.8%, and lower percentages, respectively.

The data were analyzed by expanding the yield of particles for each charge state in powers of the *pressure, corresponding to single, double, triple* collisions, etc. A first order correction for residual gas in the cell or beam line was incorporated into this analysis. A detailed description of this procedure is given in Ref. 2. For the majority of cases double and higher order collisions were negligible at the three lowest pressures used (∿ 2, 5, and 10 mTorr). However, for $q < 12$ with SF_6 gas, and for all charge states with Xe gas, the presence of double scattering events was indicated at the three lowest pressures. This introduced uncertainty into the data treatment which is indicated by parentheses around the *corresponding* cross section points in the following figures. In cases where double events were significant, no cross sections were derived. For N_2 gas, the experimental uncertainty of the cross section values σ_{4q}, $q > 4$, was found to be ∿ ±6% for $q < 12$ and ∿ ±10% for $q \geq 12$. For Ar, Kr, and Xe gas, it is ∿ ±7% for all charge states, and for SF_6 it is ∿ ±8% for the charge states $11 \leq q \leq 14$.

The method for obtaining electron loss cross sections used here is an improved version of the simple 'initial *growth*' method. The drawbacks of the simple method have been discussed by Datz *et al.*[11] but our improved method eliminates these problems. A similar data-treatment has been used previously by Heinemeier *et al.*[12]

The number of ions retaining charge state four when passing through the gas cell decreases with increasing target pressure. The cross section for loss of charge state four, $\sigma_{4,loss}$ is defined as

$$\sigma_{4,loss} = \sum_{q \neq 4} \sigma_{4,q} \,. \qquad (7)$$

It was obtained from the measured yield of 4^+ ions by fitting this yield to a straight line on a semi-logarithmic plot according to the equation.

$$Y_4 = e^{-\sigma_{4,loss}(P + P_o)} \qquad (8)$$

The procedure for determining the effective residual pressure P_o is described in Ref. 2. From the slope of the straight line, $\sigma_{4,loss}$ can be found. Experimental uncertainties associated with our measured values for $\sigma_{4,loss}$ are ±6% for N_2, Ar, Kr, and Xe, and ±15% for SF_6.

Although we did not measure the yield of particles with $q < 4$, the capture cross section σ_{43} can, in principle, be found from the experimental values of $\sigma_{4,loss}$ and σ_{4q}, $q > 4$, through

$$\sigma_{43} = \sum_{q<4} \sigma_{4q} = \sigma_{4,loss} - \sum_{q>4} \sigma_{4q} \,, \qquad (9)$$

since the cross section for double capture, σ_{42}, is probably very much smaller than σ_{43}. However, σ_{43}, obtained in this way as a difference between two large numbers, has a substantial uncertainty. Therefore, only an upper limit of its magnitude will be given here: For N_2, Ar, Kr, and Xe, σ_{43} was found to be smaller than 20% of the corresponding value of $\sigma_{4,loss}$.

The measured total cross sections *per target atom* for loss of one to eleven electrons in a single collision for 20 MeV Fe^{4+} ion transmitted through gases of N_2, SF_6, Ar, Kr, and Xe are shown in Fig. 5 as a function of the final charge state, q. For each of the target gases, the data show the same trend as a function of q: There is an overall rather steep decrease for increasing q, interrupted by a weaker decrease between $q = 6$ and $q = 8$. For the highest q-values, the cross sections follow a nearly exponential decrease with q. Defining

$$r_q = \frac{\sigma(4,q+1)}{\sigma(4,q)} \,, \qquad (10)$$

we find that r_5 (that is the ratio between the double and the single electron loss cross section) is ∿0.5 for all the target gases. Then, for example, for Kr-gas target, $r_6 \approx r_7 \approx r_8 \approx 0.7$, followed by an abrupt decrease to a value of $r_q \approx 0.4$ for $q > 8$. Comparing the results for the different gases, it is observed that the cross sections are smaller, and the decrease *at high q-values is more pronounced*, the lighter the target atoms.

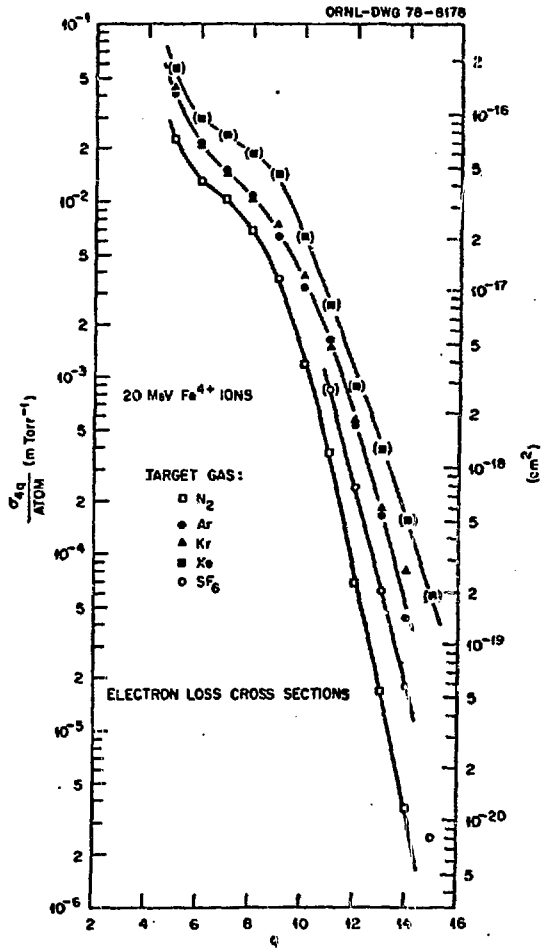

Fig. 5 - The total single and multiple electron loss cross sections, plotted as a function of the final charge state q. The gas cell length was 9.4 cm. The curves are drawn to guide the eye. The significance of data points in parentheses is discussed in the text.

The data of Fig. 5 may be compared to the results of Moak *et al.*[13] They measured electron loss cross sections for 110 MeV I^{12+} in H_2, He, and Ar and for 162 MeV I^{17+} in O_2. The 162 MeV results show a dependence of q similar to that observed in this work: The cross sections decrease steeply with increasing q, interrupted by a relatively slow decline in the region q ≈ 18 to q ≈ 25. For their 110 MeV measurements, the cross sections are very much smaller for H_2 and He and they decrease more rapidly with q than the data obtained on Ar-atoms.

Betz[4] suggested a qualitative explanation of the observed effects. He distinguishes between two basically different processes for electron loss. In the first, individual electrons are lost via a direct interaction with the target atoms. Therefore, the loss of an individual electron should occur independently of the presence of other electrons and this mechanism should apply primarily to the removal of electrons from the outer shells of the ion (low q). In the second process, the ion and the target atom form a pseudo-molecule during the collision and, through promotion and level-crossing, the ion emerges after the encounter in a highly excited and/or ionized state. The following deexcitation may cause Auger processes which lead to the removal of more electrons. This mechanism should account for the many electron loss cross sections (high q) and should be more important when more electrons are available in the pseudo-molecule. Finally Betz speculates that both mechanisms might be effective in the region of intermediate q-values, thereby causing the relatively weak decrease of the cross sections observed there. This model explains qualitatively both the q-dependence of our observed cross sections and the dependence on target atomic number. Especially, it accounts for the increasingly steep decrease of the cross sections at high q-values going from the heavy to the light target atoms as being due to the fact that the light atoms are not as effective in forming low-lying pseudo-molecular states as are the heavy target atoms.

It should be noted that the model of Betz does not explicitly involve shell effects in the explanation of the less steep part of the cross section curves. Therefore it does not readily explain the fact that the abrupt change in the slope occurs at closed shells or subshells of the ion. In this work, we find the 'shoulder' to appear at q ≈ 8 for Fe ions where the 3p subshell is closed, while Moak *et al.*[13] found it at q ≈ 25, where the M shell of the I-ions investigated in their work is closed. These shell effects point to a mechanism more directly related to the ionization potential of the highly ionized ions.

Multiple electron loss is a highly probable outcome of heavy ion heavy atom collisions. As mentioned above, we find the cross section for double electron loss to be only ∿50% smaller than the single loss cross section. Furthermore, we find the total cross section for loss of more than one electron in one collision

$$\sigma_{4,q>5} \approx \sum_{q>5} \sigma_{4q} \qquad (11)$$

to be equal to ∿1.5 times the single loss cross section for the target gases where Eq. (11) can be used, that is for N_2, Ar, Kr, and Xe.

The experimental values of the total cross sections per target atom for loss of charge state four, $\sigma_{4,loss}$, are shown in Fig. 6, plotted versus the target mean atomic number. $\sigma_{4,loss}$ is seen to increase slowly with increasing atomic number for the noble gas

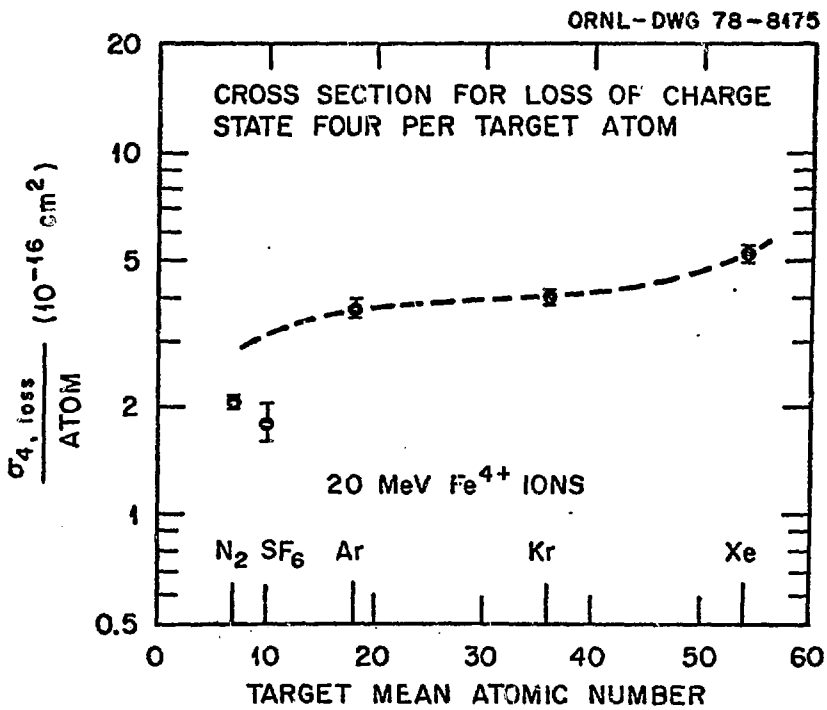

Fig. 6 - The cross sections for loss of charge state four. The dashed curve is drawn to show a possible extrapolation of the noble gas data towards lower target atomic numbers.

targets. The values for the molecular gases, however, lie somewhat lower than a smooth curve extrapolated from the heavier noble gases. This may be attributable to effects stemming from the spatial correlation between the atoms in the molecule. Similar effects have been previously seen to cause a decrease in small angle, single[14] and multiple[15,16] scattering as compared to the case of atomic target gases. These effects were investigated theoretically by Sigmund.[17]

IV. CONCLUSION

Two experimental methods, and data illustrating each, have been presented for measuring electron loss cross sections for heavy ions. Angular differential cross sections were measured for high charge states, and an analysis was made in terms of potential models. The second method used a quadrupole doublet to focus the angular distribution, and thus measure directly total cross sections. This second method has the advantage of being applicable to all charge states instead of just the high charge states, and the accuracy is better. It has the disadvantage, however, that angular information is not obtained and therefore analysis in terms of the impact parameter dependence of multiple electron loss cross sections is not possible. Thus the methods are complementary and both are useful.

REFERENCES

1. H. A. Scott *et al.*, accepted for publication in Phys. Rev. A (1979)
2. H. Knudsen *et al.*, to be published in Phys. Rev. A, March 1979.
3. V. S. Nikolaev, Usp. Fiz. Nauk 85, 679 (1965); Soviet Phys. Usp. 8, 269 (1965).
4. H. D. Betz, Rev. Mod. Phys. 44, 465 (1972).
5. G. D. Alton *et al.*, IEEE Trans. on Nucl. Sci. NS-22, 1685 (1975).
6. B. R. Appleton *et al.*, Radiation Effects 13, 171 (1972).
7. N. F. Mott and H.A.W. Massey, The Theory of Atomic Collisions (Oxford University Press, London, 1949) 1949), Second edition, Chap. VII.
8. J. Lindhard, V. Nielsen, and M. Scharff, Kgl. Dan. Vidensk. Selsk. Mat-Fys. Medd. 36, No. 10 (1968).
9. E. Everhart, G. Stone, and R. J. Carbone, Phys. Rev. 99, 1287 (1955).
10. C. D. Moak *et al.*, Nucl. Instrum. and Meth. 150, 529 (1978).
11. S. Datz *et al.*, Phys. Rev. A2, 430 (1970).
12. J. Heinemeier, P. Hvelplund, and F. R. Simpson, J. Phys. B9, 2669 (1976).
13. C. D. Moak *et al.*, Phys. Rev. 176, 427 (1968).
14. P. Loftager, private communication.
15. G. Sidenius *et al.*, Nucl. Instrum. and Meth. 134, 597 (1976).
16. F. Besenbacher *et al.*, to be published.
17. P. Sigmund, Mat. Fys. Medd. Dan. Vidsk. Selskab. 39, No. 11 (1977).